Hindawi
Geofluids
Volume 2020, Article ID 8858295, 17 pages
https://doi.org/10.1155/2020/8858295

Research Article

Insights on Climate-Driven Fluctuations of Cave ^{222}Rn and CO_2 Concentrations Using Statistical and Wavelet Analyses

Concepcion Pla [1], Angel Fernandez-Cortes [2], Soledad Cuezva [3], Juan Jose Galiana-Merino [4], Juan Carlos Cañaveras [5], Sergio Sanchez-Moral [6], and David Benavente [5]

[1] *Department of Civil Engineering, University of Alicante, 03690, Spain*
[2] *Department of Biology and Geology, University of Almeria, 04120, Spain*
[3] *Department of Biology, University of Antwerp, 2610, Belgium*
[4] *Department of Physics, Systems Engineering and Signal Theory, University of Alicante, 03690, Spain*
[5] *Department of Earth and Environmental Sciences, University of Alicante, 03690, Spain*
[6] *Department of Geology, National Museum of Natural Sciences (MNCN-CSIC), 28006, Spain*

Correspondence should be addressed to Concepcion Pla; c.pla@ua.es

Received 9 April 2020; Revised 1 June 2020; Accepted 4 June 2020; Published 27 June 2020

Academic Editor: Jinze Xu

Understanding the fluctuations in cave air concentrations and their climatic control is substantial not only to preserve the quality of indoor atmospheres but also to avoid the risk related to the presence of hazardous substances. In this study, we investigated the most influential factors affecting ^{222}Rn and CO_2 concentrations, the nature of their dynamics, and their coupling with climatic variations. For this purpose, we combined a set of mathematical methods that included a statistical and wavelet analysis of a 6-year time series in Rull Cave (Spain). Generally, the ^{222}Rn and CO_2 dynamic in cave air showed similar patterns. However, the obtained results show that these gases have a different frequency response. Thus, the annual component of ^{222}Rn and CO_2 is controlled by the relationship between external and internal temperatures. At low frequencies, both gases are affected by the same variables when the cave atmosphere reaches a minimum concentration. However, when the cave atmosphere is isolated from the outdoors, ^{222}Rn and CO_2 behave differently and disturbance caused by the visitors is evidenced in terms of the CO_2 concentration; the latter observation was confirmed by the wavelet analysis at high frequencies. In contrast, the ^{222}Rn concentration shows important variations following rainfall, which was weakly identified in the CO_2 concentration.

1. Introduction

The study of microclimate and gas composition in underground environments is critical in many investigations such as global carbon cycle, paleoclimate, geological and parietal art conservation, and health risk for guides and visitors. In particular, understanding gaseous fluctuations in indoor environments is of great importance when analyzing the possible existent health risks related to the presence of humans in these locations. Particularly, in poorly ventilated environments, this subject is critical because of the concentrations that may result in severe exposure levels for people [1, 2]. Within indoor environments, tourist caves accumulate sufficient features to be considered potential locations to be managed as indoor gas concentrations can be significant [3, 4]. For instance, there are many examples of tourist caves with high ^{222}Rn and CO_2 concentrations. Alvarez-Gellego et al. [5] reported an annual average ^{222}Rn concentration of 31.9 kBq m^{-3} in Castañar Cave, the highest radon gas concentration in a Spanish cave. In Postojna Cave (Slovenia), Gregorič et al. [6] noted maximum radon and CO_2 concentrations greater than 37 kBq m^{-3} and 4700 ppm, respectively. Fernandez-Cortes et al. [7] demonstrated that up to 5000 ppm of CO_2 were stored in the Ojo Guareña Karst system, which was characterized by large daily oscillations of CO_2 levels in caves (from 680 to 1900 ppm day^{-1} on average) caused by daily oscillations of the exterior air temperature affecting the cave air temperature. In the Lake Cave of Tapolca (Hungary), Somlai et al. [8] confirmed that the ^{222}Rn concentration could reach greater than 15 kBq m^{-3}.

Analysis of air in tourist caves is a key factor to guarantee the quality of the indoor atmosphere and that it is free of hazardous substances. Both gases, CO_2 and ^{222}Rn, affect human health differently and they should not exceed certain maximum levels. For example, an annual ^{222}Rn maximum concentration of 300 Bq m^{-3} is established in closed work environments [9]. For CO_2, the workplace long-term exposure limit (8 h) is set at 5000 ppm [10]. Consequently, the determination of factors that control gas concentration and its annual variability should be carefully performed for each indoor environment, including underground tourist caves. The ^{222}Rn concentration level depends on a complex relationship between different external and internal factors [11]. It is a decay product of radium, exhaled from certain rocks and soils. In addition, the CO_2 presence in caves is a consequence of soil activity [12–14], degasification from dripping water [15–17], and human contributions resulting from respiration [18–21]. Thus, once gases are produced, environmental factors, which control the cave atmosphere, determine the gaseous accumulation in the confined atmosphere. The porous system of the rocks and soils and the presence of water define the diffusion rates of both gases [22–25]. Diffusion is among the mechanisms responsible for gas migration and accumulation in an underground environment, and it directly depends on the physical properties of the porous materials [26–28]. In addition, the relationship between environmental factors (mostly the relationship between indoor and outdoor temperature) is responsible for the ventilation of the cave atmosphere [29–31]. The influence of factors such as the amount of rainfall [32, 33], pressure difference between the cave and outdoor atmospheres, soil temperature [34], wind gusts [35], and geomorphology [36] is a determinant in assessing the ventilation regime. Variations in cave-air ^{222}Rn and CO_2 concentrations can be interpreted together because of the relative dependence between both gases, mainly due to ventilation processes. Consequently, indoor cave concentrations depend on a balance of gaseous production and accumulation and gaseous exchange with the outdoor atmosphere.

To adopt mitigation actions in caves with high exposure levels, it is necessary to understand the main factors controlling the gaseous cave dynamics as well as determine the annual periods with the maximum gas concentration. To address this topic, complexity analyses have been performed in confined environments providing conclusive results [11, 17, 29, 37–39]. For instance, wavelet analysis [40–43], which has not been commonly employed to cave data analysis [44], was satisfactorily applied to a data period from Rull Cave [20] to differentiate the stable natural trends in cave dynamics and induced perturbations caused by visitors. In addition, multivariate statistical analysis provides a useful tool to empirically establish easy and understandable correlations between different parameters, highlighting the influence between one principal parameter and those that are related. Although these techniques have been applied to different subjects such as evaluating groundwater pollution [45], assessing the spatial and temporal trend of precipitation in a local area [46], or predicting water permeability in rocks [47], they have been discreetly applied to cave data analysis. However, recently, this type of analysis showed satisfactory results in the study of the spatial variability of cave-air carbon dioxide and methane concentrations in Gaden and Cathedral caves [35]. The main objectives of this study were to analyze the microclimatic and ^{222}Rn and CO_2 concentration time series and determine their dynamics and coupling with climatic variations in a shallow cave (Rull Cave). The key innovations introduced in this study are based in the combination of multivariate statistical and wavelet analyses to establish the structure of the variable dependence and the interrelationship and frequency response of environmental variables and gaseous concentration in subsurface environments. Although some complex statistical analyses have been previously developed in subterranean sites, the combination of the analysis presented in the present research has not been earlier implemented for the study of underground caves. To develop the analysis, first, we applied the principal component analysis (PCA) [48] for grouping the different variables in correlated ensembles during different recharge–discharge stages that Rull Cave annually undergoes. Second, stepwise multiple regression analysis was used to determine the highest weighted factors that influence ^{222}Rn and CO_2 concentrations as well as predict their concentrations during each stage. Finally, we analyzed the frequency components and their relationship with the variables in the cave atmosphere and soil-external atmospheric systems using wavelet analysis.

2. Materials and Methods

2.1. Site Information. Data collection was performed in Rull Cave (38°48′40″N, 0°10′38″W) in Vall d'Ebo (Alicante), Southeast Spain. The prevailing geological materials in the cave are both massive Miocene conglomerates and Cretaceous limestones [20, 25, 49]. The cave has a nearly round shape with a length of 1535 m and a calculated volume of 9915 m^3 [20]. In addition, there are some minor corridors surrounding the principal hall. The host rock of the cave has a variable thickness of 9 to 23 m, and in the highest level, it is located in the only entrance of the cave shut by a 3 m^2 door. CO_2 concentration in the cave is derived, mainly, from microorganisms and C3 plant growth in a silty-silty loam soil profile (approximately 1 m in thickness) developed above the cave and composed of quartz (70%), phyllosilicates (20%), calcite (5%), and feldspars (5%) [25]. C3 plants are densely distributed in the form of Mediterranean shrubs over the cave surface. The average measured $\delta^{13}CO_2$ value is -21.64‰ and -21.12‰ for the soil and cave air, respectively [49]. The predominant climate in the area is defined as a Mediterranean or warm temperate climate (Csa climate type, Koppen–Geiger Classification, [50, 51]) characterized by a dry and hot summer. For the study period (November 2012–April 2018), the average daily temperature was 15.82°C with maximum and minimum values of 35.13°C and -1.18°C, respectively. The average total annual rainfall in the study area for the same period was 410 mm. Within this period, the driest year was 2014 (248 mm) and the wettest was 2016 (635 mm).

Subsurface environments are subjected to different mechanisms that are derived from recharge, isolation, and storage processes, characterized by significant seasonal, and even daily, variations [39, 49]. In Rull Cave, four different time-dependent stages were established to perform the statistical analysis: (1) gaseous recharge, coincident with the spring and summer seasons; (2) maximum gas concentration in the cave (summer); (3) gaseous discharge (summer–autumn); and (4) a period in which the gas concentration reaches minimum values (winter).

Rull Cave is open to tourists. During the study period, 14450 people annually visited the cave, on average. Visits are not uniformly distributed in time. Maximum human perturbance occurs during March-April (Easter holiday) and August, with an average value of 74 and 92 visitors/day, respectively. In contrast, January (11 visitors/day) and February (13 visitors/day) always have the lowest number of tourist visits. Despite the human presence in the cave, microclimatic conditions are well preserved in Rull Cave, which is characterized by a thermohygrometric stability for the entire annual cycle. The average daily temperature in the cave atmosphere is 16.21°C with variations of ±0.70°C. The confined atmosphere results in humidity levels that are always near saturation (97.8%) as well as in the accumulation of both CO_2 and ^{222}Rn, which, on average, range annually from 533 to 3681 ppm and 645 to 3959 Bq m^{-3}, respectively.

2.2. Monitoring System. Environmental and microclimatic data were recorded with a monitoring system specifically installed in the cave site from November 2012 to April 2018, which was maintained and periodically revised to guarantee data quality. However, unavoidable isolated failures of the monitoring system because of the long monitoring period resulted in certain gaps in data acquisition. All measurements were performed every 30 min. Indoor conditions were monitored using a COMBILOG TF datalogger (Theodor Fiedrich & Co., Germany). The datalogger was connected to the electrical supply but also had two security batteries to ensure some autonomy. Several probes were connected to the datalogger to acquire different microenvironmental variables. Air temperature and relative humidity data were obtained using Pt100 1/10 DIN and Rotronic HygroClip S3 sensors, with measurements ranging from -40 to 100°C and 0-100% and with accuracies of ±0.1°C and ±0.8%, respectively. A CO_2 nondispersive infrared analyzer (ITR 498, ADOS; Germany) was also connected to the same datalogger to obtain cave-air concentration measurements within the range of 0-10000 ppm (0.3% accuracy). Independently ^{222}Rn measurements were taken using a Radim 5WP Radon monitor (SSM&SISIE, Prague) with an 80-50000 Bq m^{-3} measurement range. Some additional measurements were also performed with both portable and permanent independent sensors installed at some additional points of the cave, although these measurements were only employed to check the truthfulness of the data recorded at the main monitoring point as previously described. More details regarding the monitoring system can be found in [20, 25, 49]. Air temperature in the cave exterior was recorded every 30 min using a HOBO U30 Weather Station Data Logger (Onset, Bourne, MA, USA). Additionally, a 147 RG2-M rain gauge (Onset Computer Corporation, Bourne, MA, USA, resolution = 0.2 mm) was employed to measure rainfall. Finally, beginning in February 2015, soil temperature was measured using a HOBO U12 logger (Onset, Bourne, MA, USA, accuracy = ±0.35°C).

2.3. Statistical Analysis. Multivariate statistical analysis was applied to both gas concentrations (^{222}Rn and CO_2) and environmental parameters to estimate the dependencies between variables and their interrelationship using the code SPSS v.24.0 (from SPSS Inc.).

The dynamics of gas concentrations and microclimatic parameters behaved differently depending on the different stages of the cave atmosphere. As we have commented, Rull Cave has four different time-dependent stages. The beginning of stages 1 and 3 was defined by two different conditions: (i) changes in the temperature difference (ΔT) between outside (T_{out}) and inside (T_{ind}) of the cave (i.e., $\Delta T > 0$ for stage 1 and $\Delta T < 0$ for stage 3) and (ii) the existence of 10 consecutive days with an absolute variation of 200 ppm in CO_2 and 500 Bq m^{-3} in ^{222}Rn concentration. After that, stages 2 and 4 were determined by the occurrence of 10 consecutive days with an absolute variation less than 200 ppm in CO_2 and 500 Bq m^{-3} in ^{222}Rn concentration (i.e., 10 consecutive days with the persistent absence of variation in gas concentrations) (Figure 1).

^{222}Rn and CO_2 variations occurring in Rull Cave during the study period were computed as discrete events. After the evaluation of the time series, increments of 60 ppm for CO_2 and 140 Bq m^{-3} for ^{222}Rn were established as significant, considering the accuracy and measurement range of the instruments used. The selected variations in gas concentrations with all the environmentally measured variables were reported as a database (Figure 2).

PCA allows assessing variable grouping within multivariate data by the calculation of principal components for a given percentage of the total variance. These components are calculated by scores or coefficients, which incorporate the following information: (1) the absolute value of the coefficients (high values in several coefficients of the same principal component show a close relationship between them) and (2) the sign of the coefficients (the same or opposite sign of several coefficients shows the direct or inverse relationship between them, respectively). PCA was performed using Varimax as a factor rotation method. In this analysis, the employed variables were ^{222}Rn and CO_2 concentrations, indoor environmental variables (cave temperature and relative humidity, T_{ind}, and RH_{ind}), visitors, and atmospheric variables (rainfall, outdoor temperature (T_{out}), and soil temperature (T_{soil})).

Multiple linear regression analysis was carried out to quantify the associations established in the PCA for each stage. For this analysis, CO_2 and ^{222}Rn act as dependent variables using the previously defined database (increments

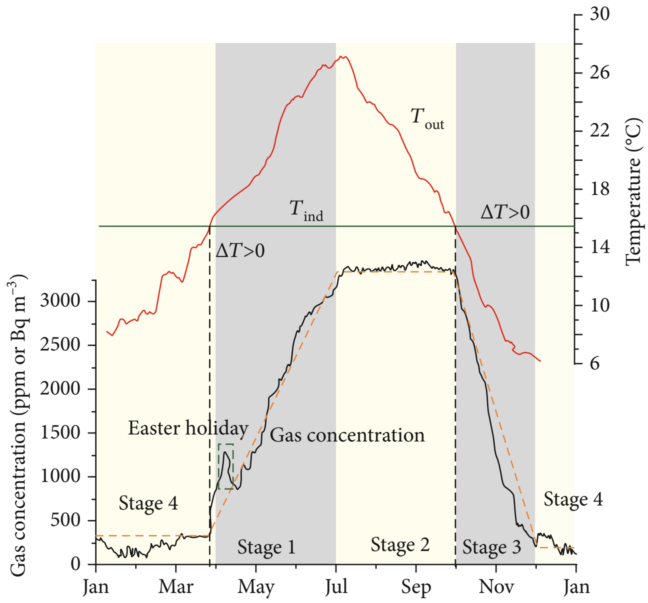

FIGURE 1: Delimitation of the different stages to perform the analysis. Indoor and outdoor temperatures and gas concentration do not represent real values but are an example for illustration.

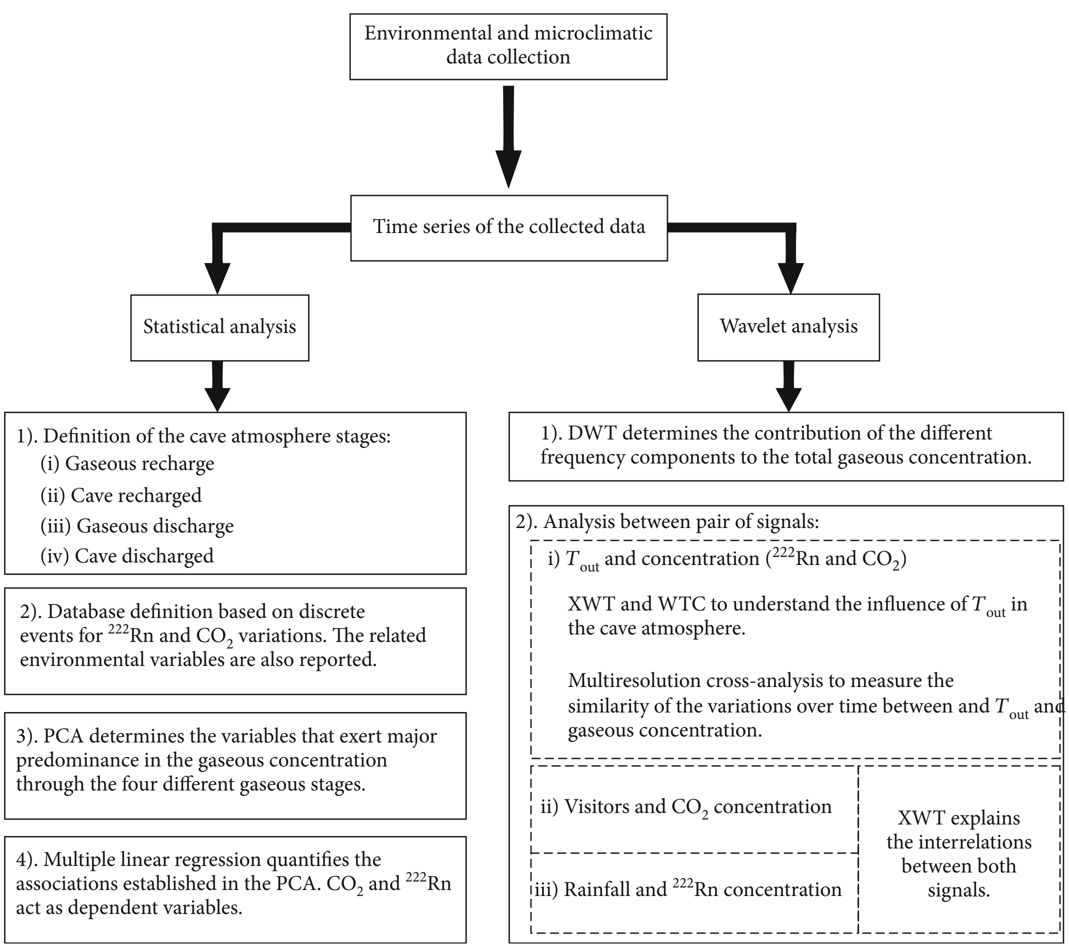

FIGURE 2: Workflow of the methodology applied to the data.

equal or greater than 60 ppm for CO_2 and 140 Bq m^{-3} for ^{222}Rn). They were computed together with the environmental parameters (rainfall, visitors, T_{ind}, T_{out}, T_{soil}, and RH_{ind}), which act as independent variables in the multiple linear regression analysis. This analysis also included the weight (magnitude of the standardized coefficients) of each independent variable in the calculation of multiple linear equations and therefore quantified the influence of each variable in the variation in gas concentrations during each stage (Figure 2).

2.4. Wavelet Analysis Applied to the Time Series. Aiming to establish the contribution of the different variables to the gas concentrations in the cave, recorded climatic signals were individually decomposed using the wavelet analysis [40–43]. Discrete wavelet transform (DWT), using Daubechies 5 as a mother wavelet, was employed to differentiate the different frequencies (or periodicities) contained in the analyzed signals through a complete time-frequency analysis (Figure 2). The distinction of the different frequencies of the signal allows differentiating the contribution of these components (daily, intermediate, and annual) to the real recorded signal. This analysis was developed using the Environmental Wavelet Tool (EWT) MATLAB-based code [44], in which the package developed by Grinsted et al. [52] was incorporated. The EWT was previously employed in similar analyses [20, 53] offering accurate results. In addition to the particular decomposition of the individual signals, cross wavelet transform (XWT) and the wavelet transform coherence (WTC) were implemented between the pair of signals (one being the gas, CO_2, or ^{222}Rn concentration) to understand the influence of the individual variables in the cave atmosphere (Figure 2). Results of this analysis were evaluated through the interrelations between two time-domain signals (explained by the XWT) and the coherence between them (WTC), resulting in the identification of areas with high common power in the final scalograms [52]. Finally, to conclude the analysis and with the aim of measuring the similarity of the variations over time between two signals [54], a multiresolution cross-analysis was also performed between them [55, 56]. The analysis results in values between −1 and 1, with higher correlation coefficients showing higher similarity between the analyzed signals.

3. Results and Discussion

3.1. Frequency Response of ^{222}Rn and CO_2 Time Series. Figure 3 shows the temporal evolution of gas concentrations and microclimatic parameters in the cave and soil and the external weather conditions from December 2012 to April 2018. The recorded time series also includes the daily visitors. Rull Cave atmosphere shows the typical thermohygrometric stability observed in shallow caves [22, 30, 49]. The cave atmosphere temperature and humidity are very stable with an annual variability of ±0.7°C for temperature and 3.1% for relative humidity. In addition, ^{222}Rn and CO_2 concentrations show distinguishable seasonal and nearly regular cycles, similar to the outdoor temperature. The key factor to understand the influence of each variable is to consider that the gas concentrations of ^{222}Rn and CO_2 are the result of the interaction of different components that prevail under different periodicities [17, 20, 57, 58].

Interannual variation of CO_2 and ^{222}Rn depends mostly on the relationship between outdoor and cave temperatures which establishes the beginning and the end of the gaseous recharge and, in turn, the length of the different annual cycles of gaseous concentration. The beginning and end of the gaseous recharge and discharge also establish the annual periods in which the cave is recharged and discharged. Interannual differences in CO_2 cave concentration also depend on CO_2 soil concentration, which is affected by soil temperature and water content. Outdoor temperature influences soil temperature whereas soil water content is related to rainfall. Consequently, interannual rainfall variations exert their influence in the gaseous concentration [20, 49].

Variations of CO_2 and ^{222}Rn at lower frequencies (daily to annual) are evaluated in the present study. The ^{222}Rn and CO_2 time series can be decomposed into different components following different multiresolution levels corresponding to daily, intermediate (from a week to a few months), and annual periodicities.

There are some differences between the frequency decomposition of both signals (Figure 4). The different components of the time series (daily, intermediate, and annual) extracted when filtering the signal using wavelet analysis show different contributions to the total registered concentration. While the major contribution of both gases corresponds to the annual component (i.e., the one directly dependent on the relationship between external and internal temperatures), ^{222}Rn measurements show larger contributions of daily and intermediate components. For ^{222}Rn (Figure 4(a)), the annual component contributes a maximum of 3770 Bq m^{-3} (depending on the evaluated year). Average values of the annual component suppose a contribution greater than 87.8% of the total ^{222}Rn amount in the cave (Figure 4(a)). The annual component contribution is similar for CO_2 (maximum of 3752 ppm; Figure 4(b)) and also depends on the annual cycle. The intermediate component for ^{222}Rn results in continuous oscillations in the cave concentration, with maximum values greater than 802 Bq m^{-3}. Average values of the intermediate ^{222}Rn component suppose 9.3% of the total ^{222}Rn concentration. Although the contribution of the average values of the daily component to the global ^{222}Rn concentration is smaller (nearly 3.0%), it can modify the cave atmosphere by up to 443 Bq m^{-3} when maximum values occur. The component of intermediate frequencies in CO_2 shows a maximum variation in the concentration of 846 ppm, but these events are scarcer through the time domain. The maximum value detected of the daily component of CO_2 supposed an increase of 275 ppm in the gas concentration. Average values of this daily component suppose a contribution to the global CO_2 concentration of 1.3% (Figure 4(b)).

3.2. Determination of Control Parameters in the Cave Gaseous Atmosphere. PCA considered the database for the four different gaseous stages that Rull Cave undergoes

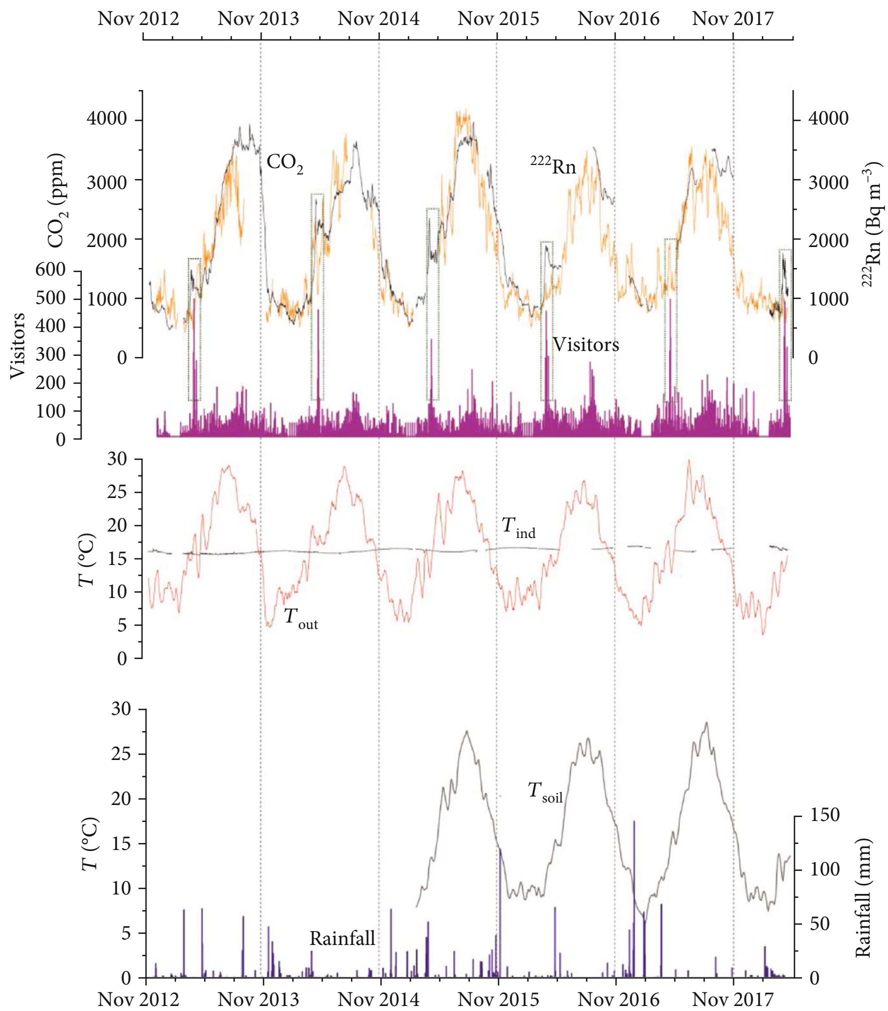

Figure 3: Temporal evolution of microclimatic variables in Rull Cave for the period December 2012-April 2018. Measured variables are as follows: CO_2 (ppm) and ^{222}Rn (Bq m^{-3}) concentrations; outdoor (T_{out}), cave (T_{ind}), and soil temperature (T_{soil}) (°C); visitors; and daily rainfall (mm). The presence of visitors during Easter holiday for each year of the time series is marked with rectangles in dashed lines.

(Figure 1). This analysis shows, within each stage, the group of variable changes that exerts major (linear) predominance in the cave gas composition (Table 1).

Gaseous recharge in the cave (stage 1) simultaneously occurs with increases in the outdoor temperature. ^{222}Rn accumulates in the cave because of the relationship between the temperatures, which is responsible for the isolation of the cave atmosphere, allowing the ^{222}Rn concentration to increase. Consequently, T_{out}, T_{soil}, and, inversely related, RH_{ind} appear in Component 1 with this gas. However, the absence of CO_2 in this component is remarkable. Although the general trend of Rull Cave shows simultaneous increases in both gases (^{222}Rn and CO_2), the presence of an important number of visitors during the Easter holiday is predominant in determining the CO_2 concentration in the cave (Figure 3), and consequently, Component 3 demonstrates this significant influence of visitors on CO_2 concentration. In Component 2, the presence of a high coefficient for rainfall and indoor temperature might be related to the fact that these variables are not the principal parameter in determining Rull Cave gas concentration during this stage. In addition, the dry conditions outdoors establish this variable grouping.

When the cave reaches its maximum gas concentration (stage 2), continuous tourist visits that occur during the summer (Figure 3) have an important influence on CO_2 concentration and cave temperature (Component 2). During this stage, air renewal in the cave atmosphere is nearly nonexistent causing cumulative effects of an increase in CO_2 concentration and cave temperature as a consequence of the visitors. This might be the most influential factor in CO_2 concentration increases in the cave. Meanwhile, the ^{222}Rn concentration is directly related to outdoor temperature variations (Component 1). Although environmental parameters also affect the CO_2 concentration, the high visitation during stages 1 and 2 triggers the component grouping for these stages. When the gas concentration (stage 3) starts decreasing in the cave atmosphere, both gases are matched in Component 1. The gas concentration simultaneously decreases for both gases because of new air mass movements resulting from indoor and outdoor air densities affected by changes

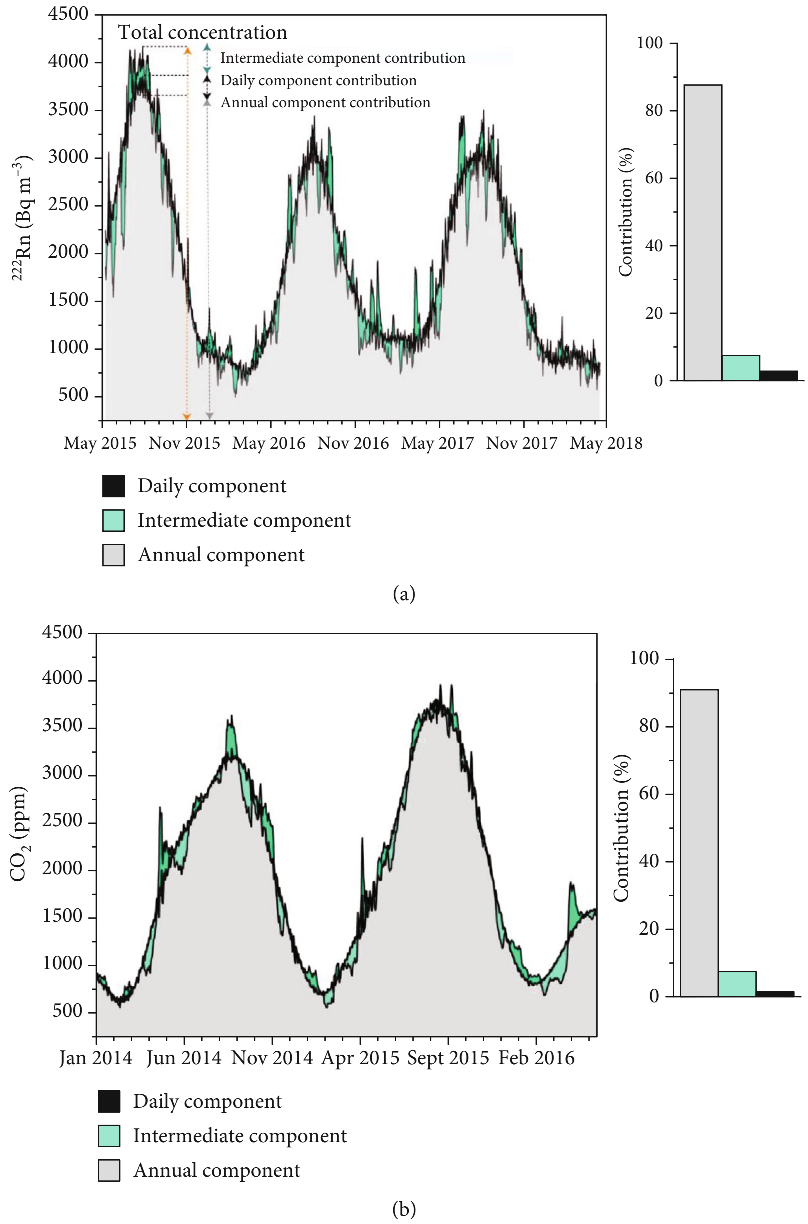

Figure 4: Contribution of the different frequency components (annual, intermediate, and daily) to the global gas ^{222}Rn (a) and CO_2 (b) concentrations. The subfigures are not coincident in the time domain because they represent the maximum available continuous measurement range with the absence of missing data.

in their temperatures. Component 1 also shows an inverse relationship between number of visitors and gas concentration. During this stage, the isolation of the cavity decreases. In addition, when visitors (there are few during this stage) access the cave, the cave's door is open and, consequently, the gas concentration may slightly decrease. Finally, stage 4 is marked by a gaseous discharged atmosphere in which mass air movements are predominant and cause ventilation episodes with the lowest degree of isolation during the annual cycle. Consequently, ^{222}Rn and CO_2 behave similarly, affected by variations in indoor temperature and relative humidity, and they are not influenced by the presence of visitors. Component 2 explains the ^{222}Rn and CO_2 variations because of the high ventilation rates in the cave atmosphere.

Results from PCA allow establishing gas concentration from the most influential variables calculated for each stage. Respectively, as shown in Figures 5 and 6, ^{222}Rn and CO_2 concentrations act as dependent variables estimated by multivariate analysis as a combination of the independent variables established in the PCA grouping (Table 1).

The goodness-of-fit of the ^{222}Rn and CO_2 concentrations shows proper accuracy as demonstrated in most cases by the correlation coefficients obtained for each analysis which varies from 0.4660 to 0.9071. Changes in cave behavior are highlighted in the previous analysis in which the predominant variables in determining the cave gas concentration change depending on the cave stage. Relations between outdoor and indoor temperatures are always present within the

TABLE 1: Results of variable grouping from PCA considering the different stages that Rull Cave undergoes.

Cave atmosphere stage	Variables	Component 1	Component 2	Component 3
1 (gaseous recharge)	Rainfall	-0.149	*-0.953*	-0.163
	Visitors	0.253	-0.353	*0.850*
	CO_2	-0.269	0.453	*0.806*
	^{222}Rn	*0.757*	0.162	0.077
	T_{ind}	-0.122	*0.922*	-0.285
	T_{out}	*0.857*	-0.042	0.080
	T_{soil}	*0.653*	0.451	-0.555
	RH_{ind}	*-0.883*	0.238	0.190
% explained variance	86.26	33.60	29.70	22.96
2 (cave recharged)	Rainfall	*-0.756*	0.065	-0.080
	Visitors	0.079	*0.852*	-0.080
	CO_2	0.291	*0.543*	-0.318
	^{222}Rn	*0.743*	0.434	0.118
	T_{ind}	-0.112	*0.904*	0.066
	T_{out}	*0.763*	-0.364	-0.323
	T_{soil}	*0.882*	0.234	0.090
	RH_{ind}	0.122	-0.091	*0.940*
% explained variance	74.46	32.53	27.82	14.11
3 (gaseous discharge)	Rainfall	0.057	-0.002	*0.998*
	Visitors	*-0.948*	0.053	-0.281
	CO_2	*0.916*	-0.222	-0.333
	^{222}Rn	*0.843*	0.418	0.106
	T_{ind}	*-0.938*	-0.199	0.049
	T_{out}	-0.260	*0.913*	0.311
	T_{soil}	0.264	*0.910*	-0.317
	RH_{ind}	*0.976*	-0.160	-0.036
% explained variance	97.21	55.29	24.43	17.48
4 (cave discharged)	Rainfall	*0.770*	0.308	(only two components in stage 4)
	Visitors	*-0.893*	0.091	
	CO_2	-0.467	*0.827*	
	^{222}Rn	0.592	*0.745*	
	T_{ind}	0.437	*0.748*	
	T_{out}	*0.969*	0.214	
	T_{soil}	*0.899*	-0.137	
	RH_{ind}	-0.031	*0.975*	
% explained variance	85.16	48.70	36.45	—

entire annual cycle as demonstrated by the presence of these variables (T_{ind}, T_{out}, or even T_{soil}, which is dependent) in the multivariate analysis. During gaseous recharge and once the cave is recharged (stages 1 and 2), the relationship between outdoor and cave temperature determine the ^{222}Rn and CO_2 accumulation. The isolation of the cave atmosphere, which is calm during these stages, results in a major influence of visitors on the CO_2 concentration (Figures 6(a) and 6(b)). The discharge period is described by less isolation of the cave atmosphere with a predominance of air mass movements as a consequence of changes between the temperature relations (T_{out} and T_{ind}). Scarcer changes in the gas concentrations are simultaneous because of the involvement of the same variables (Figures 5(c), 5(d), 6(c), and 6(d)).

Results from PCA and multiple linear regression analysis demonstrate that the relation between temperatures ($T_{out} - T_{ind}$) is always present in the determination of cave gas concentration. Furthermore, the presence of visitors has

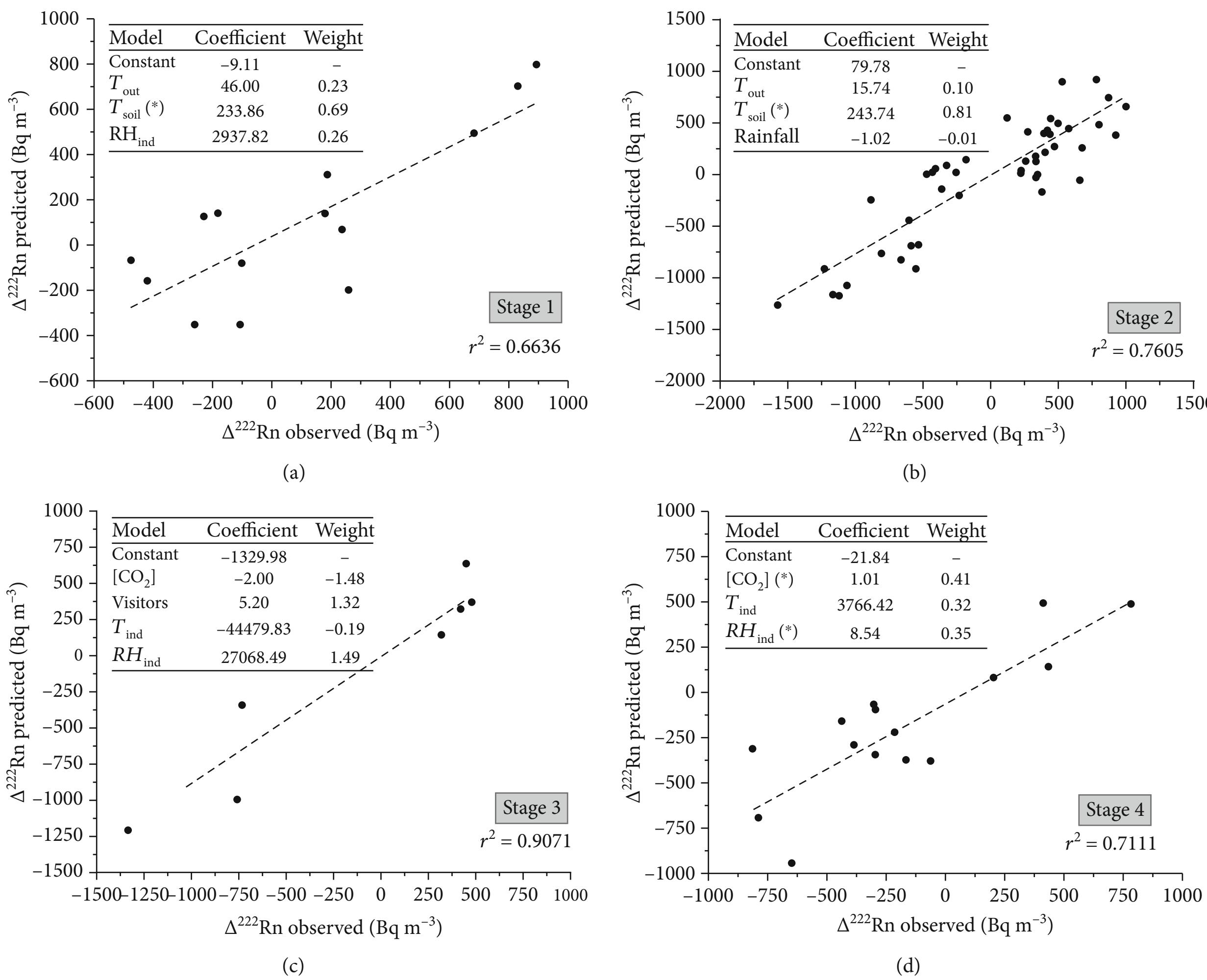

Figure 5: Observed and predicted values of ^{222}Rn increments considered for the different cave stages: (a) stage 1 (gaseous recharge), (b) stage 2 (maximum gas concentration in the cave), (c) stage 3 (gaseous discharge), and (d) stage 4 (minimum gas concentration in the cave). Predicted values are obtained in each case considering the predictor variables established in the PCA (Table 1). The unstandardized coefficient (coefficient) of each predictor variable within the multivariate analysis as well as its weight (standardized coefficient) is shown for each individual prediction. * indicates significant variables in the multivariate analysis.

been highlighted as among the most influential variables during some of the gaseous stages of Rull Cave. Although rainfall only appears as a control parameter in one of the performed multivariate analysis, its influence on the gaseous atmosphere in Rull Cave has been previously demonstrated [25, 49]. However, it is likely that the rainfall behavior in the study area (it is scarce and irregularly distributed in time because of the semiarid climate; Figure 3) results in the multivariate analysis not properly reflecting the influence of this variable in the cave gas concentration. Consequently, the influence of the previously mentioned variables (temperature, visitors, and rainfall) needs a particular analysis and will be individually analyzed next.

3.3. Individual Analysis of Control Parameters in the Cave Gaseous Atmosphere

3.3.1. Temperature. Time series data indicate that the variation in both gases, ^{222}Rn and CO_2, is a consequence of the temperature difference ($T_{out} - T_{ind}$) variation at an annual scale. As previously demonstrated, this is among the most influential parameters, which establishes the seasonal component of both signals. The indoor temperature varies within a range of ±0.7°C, which supposes a small percentage considering the annual variation of the outdoor temperature (nearly 22°C). For this reason, the influence of variations in the temperature gradient between the exterior and cave air can be evaluated by studying the outdoor temperature variation, as confirmed by the wavelet analysis. Both gases, ^{222}Rn and CO_2, reach a maximum concentration during the warmer months. The entrance of external air (with a low CO_2 and ^{222}Rn concentration) by an advective process significantly decreases the cave air gas concentrations during the coldest periods.

Individual analysis of the different signals (Figure 7(a)) establishes the different predominant periodicities for the entire evaluated period. CO_2 and ^{222}Rn behavior coincides at lower frequencies: the seasonality within the 1-year band

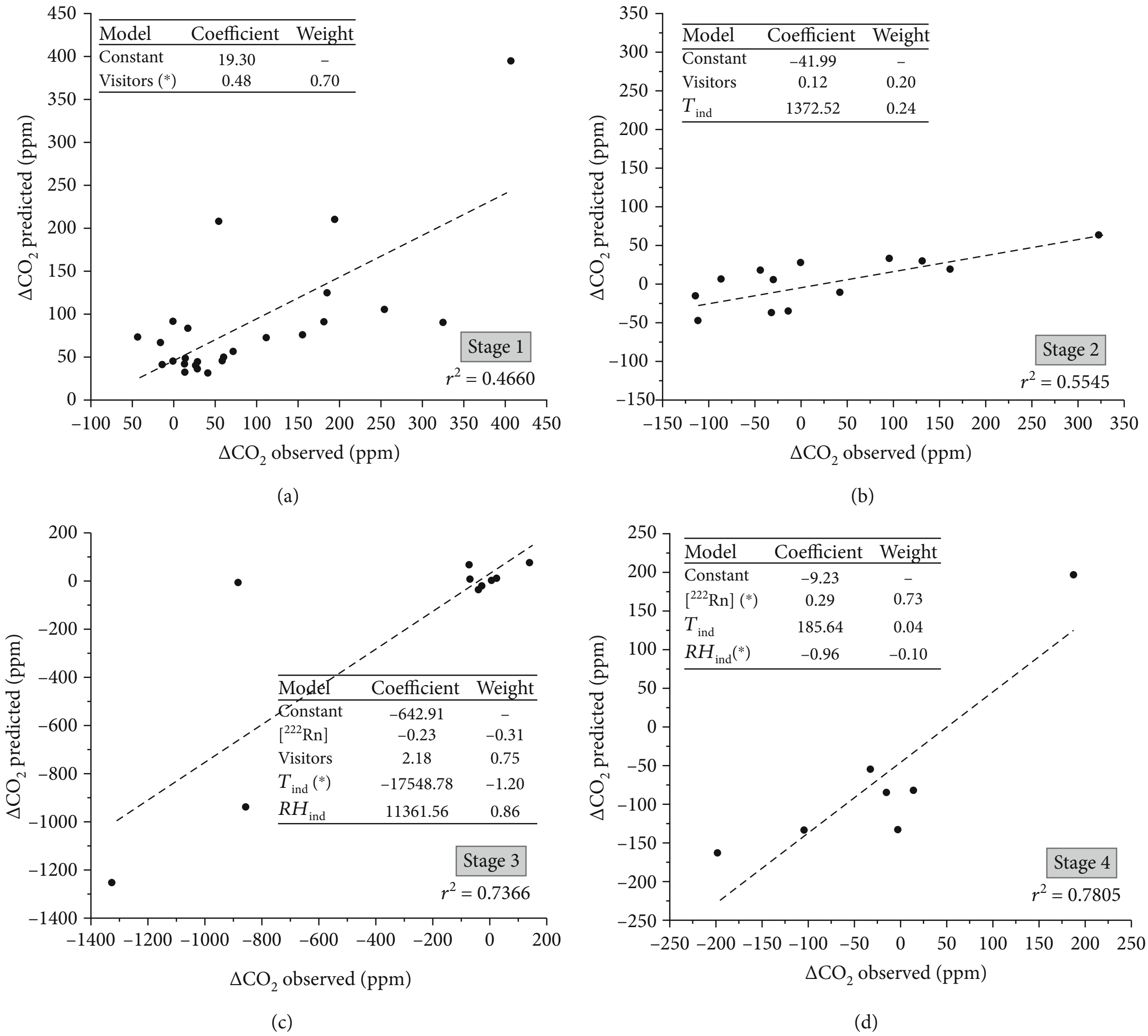

FIGURE 6: Observed and predicted values of CO_2 increments considered for the different cave stages: (a) stage 1 (gaseous recharge), (b) stage 2 (maximum gas concentration in the cave), (c) stage 3 (gaseous discharge), and (d) stage 4 (minimum gas concentration in the cave). Predicted values are obtained in each case considering the predictor variables established in the PCA (Table 1). The unstandardized coefficient (coefficient) of each predictor variable within the multivariate analysis as well as its weight (standardized coefficient) is shown for each individual prediction. * indicates significant variables in the multivariate analysis.

is always highlighted with the 1-year band periodicity strongly marked. In addition, the daily periodicity of temperature is clearly marked within the 1-day band. CO_2 and ^{222}Rn daily variations reflect that gases are also sensitive to temperature changes at higher frequencies (1-day periodicities; better reflected for ^{222}Rn). Thus, temperature changes are the most important variable to establish the seasonal (annual) pattern of the gases as indicated by the higher energy (red colors) present in this band. The analysis of WTC and XWT (Figures 7(b) and 7(c)) demonstrates the existing phase relation (arrows pointing right) between the outdoor temperature and gas concentration considering the annual periodicity reflected by the different analyzed cycles. There are also some phase relations between both gases and outdoor temperature that appear at daily and intermediate periodicities although they are lower than those in the annual band. This fact confirms that gaseous variations at high frequencies are also dependent on other environmental variables.

Multiresolution cross-analysis shows that the highest cross-correlation (Figure 8) (0.84 for ^{222}Rn and 0.78 for CO_2) occurs for the annual periodicity (annual-seasonal resolution) such that the studied times series mainly covary in the low-frequency domain (i.e., annual variations). Rull Cave undergoes annual periodic cycles in which ^{222}Rn and CO_2 describe the same pattern even when the source of the gases is different. On the one hand, ^{222}Rn is a radioactive gas with a half-life of 3.8 days and a decay product of ^{226}Ra. It is released from minerals of soils and rocks into their pore space and then to the underground atmosphere. On the other hand, CO_2 is produced in soil and, following its production, flows through the pore system of soils and rocks to the cave atmosphere. A supplementary contribution of cave CO_2 is

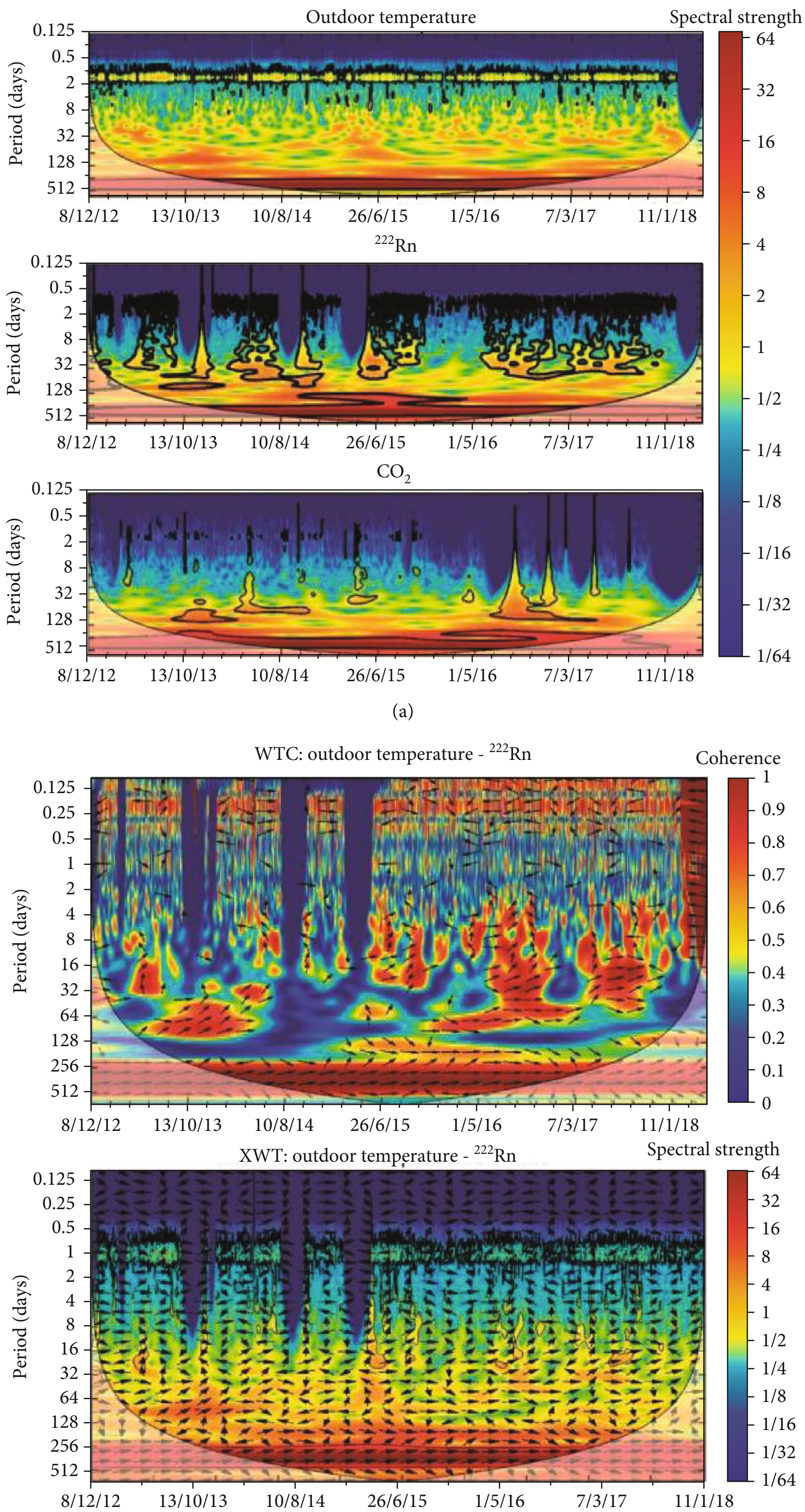

Figure 7: Continued.

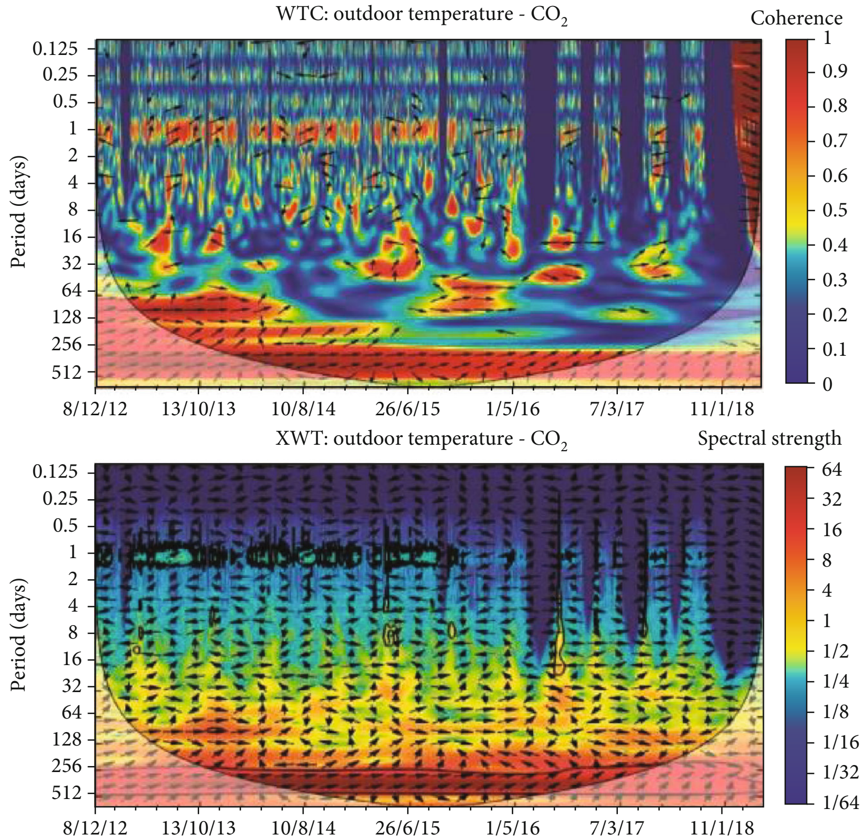

(c)

FIGURE 7: (a) Decomposition of different periodicities for outdoor temperature, ^{222}Rn, and CO_2. (b) WTC and XWT between outdoor temperature and ^{222}Rn. (c) WTC and XWT between outdoor temperature and CO_2; spectral strength and coherence range from blue (weak) to red (strong) colors. Arrows indicate the relative phase relationship (inphase pointing right, antiphase pointing left, one signal leading the other by 90° pointing up/down). Curved lines on scalograms indicate the cone of influence where the edge effects are important.

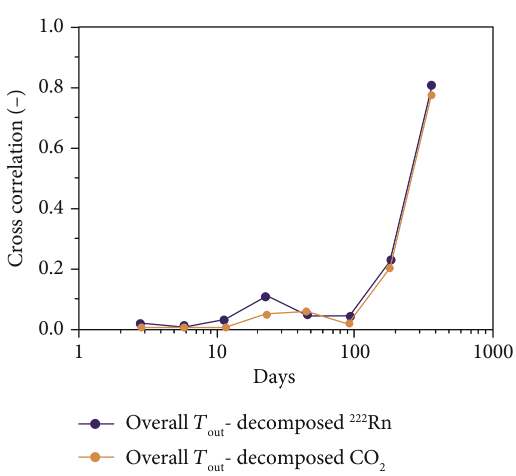

FIGURE 8: Cross-correlation function between outdoor temperature and decomposed ^{222}Rn and CO_2 at different multiresolution levels.

anthropogenic production, which occurs in tourist caves such as Rull Cave (Figure 6). This multiresolution analysis does not show important correlations out of the annual periodicity, which is probably related to the major influence of this annual periodicity.

Annual gas concentration is subject to two outstanding phenomena related to the thermal relationship between the outdoor and indoor air temperatures. This relationship directly determines the cave ventilation intensity [59–61] in which diffusive and advective fluxes occur. Changes in the relationship between outdoor and indoor temperatures constantly affect the gas concentrations through advective processes but, simultaneously, diffusive fluxes also occur from the epikarst to the cave. During an annual cycle, during stage 1, T_{out} exceeds T_{ind}, which causes a pause in the ventilation process and thus in the predominance of diffusive fluxes because of the isolation of the cave atmosphere as a consequence of the density difference between the air masses. This is clearly confirmed by the wavelet analysis with the 1-year band dependent on the temperature variation. When the temperature gradient ($T_{out} - T_{ind}$) is inverted, the stored volume of gases depends on multiple variables, which might be different for each gas. Consequently, these transient changes in the ventilation state influence the ^{222}Rn and CO_2 concentrations affected by different procedures characterized by higher frequencies (lower periodicities). Variations of a high-frequency component of temperature may occur as consequence of the visitors in the cave who also affect the high-component CO_2 signal (Figure 7).

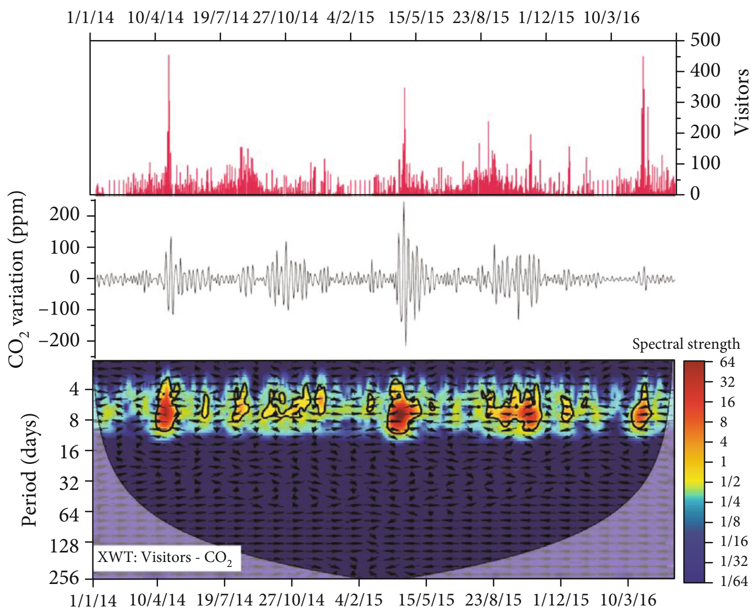

Figure 9: Energy across the multiresolution level corresponding to the 4-16 days of CO_2 and visitors. XWT between visitors and CO_2 at high frequencies; spectral strength ranges from blue (weak) to red (strong) colors. Curved lines on the scalograms indicate the cone of influence where the edge effects are important.

3.3.2. Visitors. The impact of visitors on the gas concentration in Rull Cave is strongest when the cave atmosphere has the maximum degree of isolation (i.e., during stages 1 and 2; Table 1, Figure 9). These results are coincident with multivariate analysis (Figure 6). The entrance of (many) visitors in the cave particularly affects CO_2 and markedly varies its high-frequency band, mainly during stages 1 and 2. High visitation during stages 1 and 2 may alter the CO_2 regime, but because it does not occur every day (visits are particularly concentrated on the weekends and bank holidays), CO_2 variations because of visitors are not daily occurrences. In addition, annually and once a week, the cave receives one larger group. For this reason, the periodicities of the interaction between CO_2 and visitors are mostly concentrated in the 4-16-day band. The energy across the multiresolution level corresponding to the 4-16-day band is high as indicated by the CO_2 variations (on occasions greater than 250 ppm) when large groups of people visit the cave. Energy variations in CO_2 show fluctuations, which are consistently, mainly, associated with the presence of visitors.

PCA results establish that the effect of visitors on the ^{222}Rn concentration occurred mainly during stage 3. However, wavelet analysis did not detect changes in the ^{222}Rn concentration because of the presence of visitors: energy levels did not show matches between the gas variations and human presence. These results confirm that the number of visitors is not a suitable variable to evaluate changes in the ^{222}Rn concentration. To perform an accurate analysis, it will be necessary to compile a comprehensive record of the periods in which the cave door is open to relate the effect of visitors on the ^{222}Rn concentration.

3.3.3. Rainfall. Although the multivariate analysis did not show a substantial influence of rainfall on ^{222}Rn and CO_2 concentrations, rainfall is among the variables that contribute to the increase in gas concentrations in the cave. Two main factors may increase the cave gas concentration. On the one hand, a piston effect occurs at the beginning of rainfall [62]. Gas concentrations stored in the voids of the soil and rock porous system are pushed into the cave. If the rainfall occurs outside of the recharge period, this effect is highlighted, because the concentrations in the porous system are higher than those in the cave. This effect is noticeable the first time there is a break in rainfall. However, after the washing effect produced by rain, water fills the pore space and avoids the cave degasification, as the gases are retained. On the other hand, rainfall water dissolves the gases accumulated in the soil and transports them into the cave. When the water enters the cave, degasification contributes to increases in the gas concentration.

Wavelet analysis demonstrates that rainfall and ^{222}Rn show a similar behavior in the high-frequency band. Analysis developed from May 2015 to April 2018 (a set of data with no missing data) demonstrates that the relationship between both signals appears at intermediate frequencies when a rainfall occurs. However, the direct influence of rainfall on the CO_2 of Rull Cave has not been detected neither from wavelet analysis nor from PCA–multivariate analysis for the studied period. Within the period from May 2015 to April 2018, three important rainfall episodes of greater than 50 mm occurred during October-November 2015, April 2016, and November 2016, which affected the ^{222}Rn concentration in the cave and which are identified in the 4-32-day period band (Figure 10).

Two different rainfall episodes were specifically analyzed. First, during April 2013 (Figure 11(a)), after a rainfall episode of 99.2 mm, the ^{222}Rn concentration in the cave increased by 449 Bq m^{-3}. This rainfall episode was followed by some days

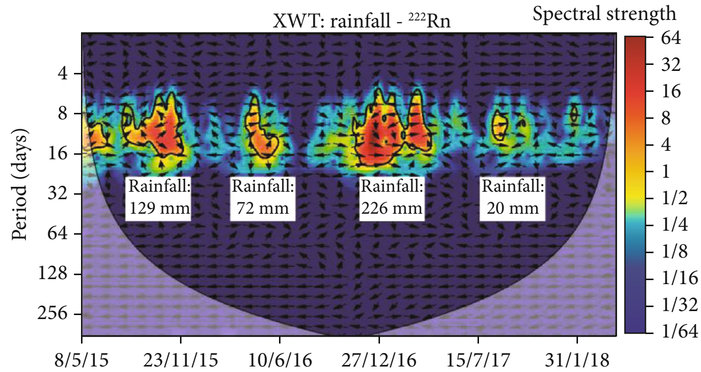

Figure 10: XWT between rainfall and ^{222}Rn at high frequencies; spectral strength ranges from blue (weak) to red (strong) colors. Curved lines on the scalograms indicate the cone of influence where the edge effects are important.

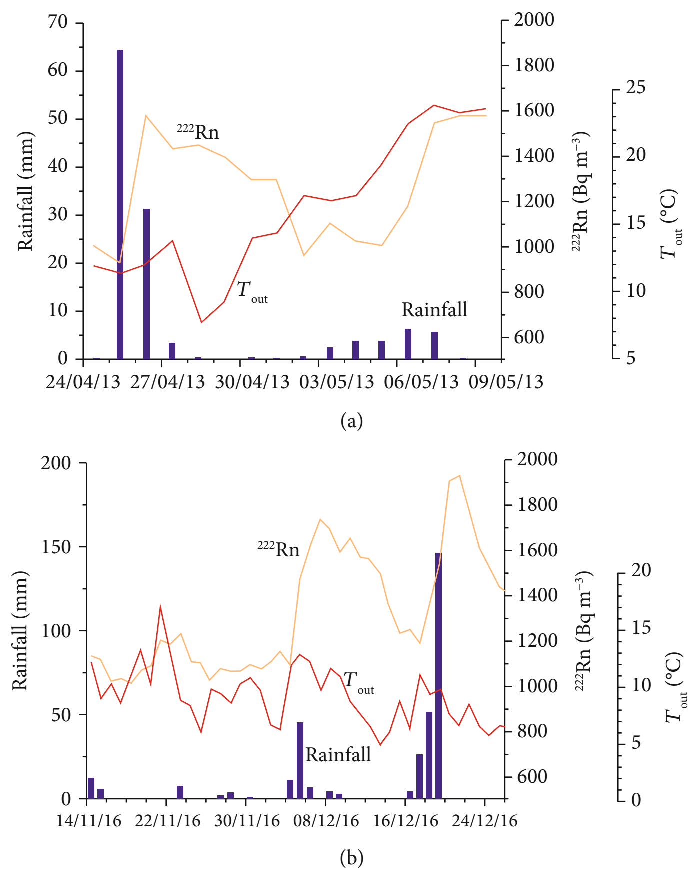

Figure 11: Detail of the increase in ^{222}Rn concentration during (a) April 2013 and (b) November 2016.

without precipitation and then by consecutive wet days when the ^{222}Rn showed a new increase. Second, during December 2016 (Figure 11(b)), rainfall occurred for four consecutive days with a total amount of 226 mm. Because of this rainfall, the ^{222}Rn concentration in the cave increased by 580 Bq m^{-3}. Rainfall contributes to variations in the ^{222}Rn concentration at intermediate and nearly daily periodicities because it always occurs on various days. For instance, the episode that occurred during December 2016 lasted 15 days. The effect of the temperature variation can be discarded during the rainfall of November 2016. In April 2013, there was an increase in outdoor temperature, but it was not synchronous with the gas concentration increase. Thus, the increase in ^{222}Rn concentration here was directly related to the rainfall event.

A nearly instantaneous increase in ^{222}Rn concentration was detected as consequence of a rainfall event. For the entire study period (November 2012-April 2018), there were 12 significant rainfall episodes with greater than 50 mm, although only 9 of them had a ^{222}Rn measurement. Results show that the amount of precipitated water determined the increase in ^{222}Rn concentration. Triggered rainfall values, ranging from 80 to 100 mm, are needed to cause a significant ^{222}Rn

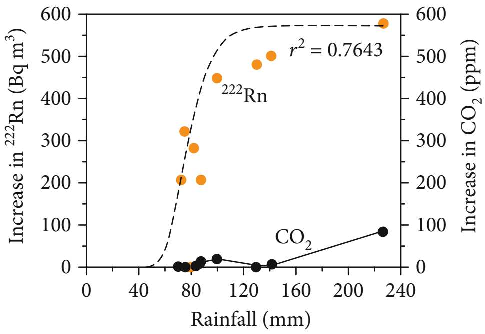

Figure 12: Variation in ^{222}Rn (Bq m^{-3}) and CO_2 when rainfall occurs. Study period: November 2012-April 2018. ^{222}Rn data fits to a Gompertz function with a critical size threshold of 77 mm.

increment. A sigmoidal Gompertz curve establishes that the trigger rainfall value is centered on 77 mm (Figure 12). However, on average, rainfalls greater than 100 mm produce increases in concentration varying from 400 to 600 Bq m^{-3}. The study reveals that ^{222}Rn reaches its maximum concentration in the cave atmosphere when a rainfall of around the trigger value defined by the model occurs. But from this rainfall value, ^{222}Rn does not show increases although rainfall exceeds it. In contrast, variations in CO_2 concentration do not show the same behavior because CO_2 is only affected by very high rainfall (Figure 12). Moreover, the wavelet analysis with CO_2 and rainfall was inconclusive and its increase after a rainfall episode was not as noticeable as that of ^{222}Rn (Figure 10).

4. Conclusions

Determination of the factors that control the gas concentration in caves as well as the evaluation of the variability at different frequencies is important to preserve the quality of indoor atmospheres and avoid the risk related to the presence of hazardous substances. Thus, a comprehensive analysis of these factors is required for each indoor environment. In Rull Cave, ^{222}Rn and CO_2 concentrations depend on complex relationships between different external and internal factors.

For that purpose, we combined multivariate statistical and wavelet analyses. Wavelet analysis provided the decomposition at different multiresolution levels (daily, intermediate, and annual periodicities) of the gas concentration and environmental variables. This analysis concluded that ^{222}Rn and CO_2 have a different frequency response. In Rull Cave, the annual component of both gases, ^{222}Rn and CO_2, corresponds to the major contribution of the total concentration and is controlled by the relationship between external and internal temperatures. However, intermediate and daily oscillations are also of great magnitude. For instance, the daily component of ^{222}Rn can modify the cave atmosphere by up to 443 Bq m^{-3}.

The variable grouping of the parameters established with PCA shows that when the cave is isolated (stages 1 and 2), increases in ^{222}Rn are dependent on temperature changes and relative humidity. This analysis also concluded that, in addition, CO_2 is determined by these factors but the presence of visitors during this period has a stronger effect on its concentration. In contrast, when the cave had the minimum concentrations, both gases are affected by the same variables.

The proposed methodology, combining multivariate analysis and wavelet analysis, highlighted the annual dependency of gas concentration on the temperature gradient ($T_{out} - T_{ind}$) and its influence in the predominance of gaseous diffusion or advection. In addition, the energy fluctuations of the wavelet analysis confirmed the influence of the presence of visitors on the CO_2 concentration defined as high-frequency perturbations. The rainfall influence on the gas concentration of Rull Cave is perfectly defined for ^{222}Rn with a nearly instantaneous increase in this gas following a rainfall occurrence. On average, rainfalls greater than 100 mm produce increases in concentrations varying from 400 to 600 Bq m^{-3} whereas CO_2 is only affected by very high rainfalls.

Results obtained from this study evidence that the combination of multivariate statistical and wavelet analyses successfully established the structure of the variable dependence and their interrelationship and frequency response. We consider that this methodology can be applied to any other investigations in a cave atmosphere–soil–external atmosphere system.

Data Availability

The raw data of the statistical analysis performed in this study are available from the corresponding author upon request.

Conflicts of Interest

There are no conflicts of interest to declare.

Acknowledgments

This research was funded by the Spanish Ministry of Science, Innovation and Universities (projects CGL2016-78318-C2-1-R, CGL2016-78318-C2-2-R, and RTI2018-099052-B-I00) and the University of Alicante (project GRE17-12).

References

[1] D. Benavente and C. Pla, "Effect of pore structure and moisture content on gas diffusion and permeability in porous building stones," *Materials and Structures*, vol. 51, no. 1, p. 21, 2018.

[2] A. Moreno-Rangel, T. Sharpe, F. Musau, and G. McGill, "Field evaluation of a low-cost indoor air quality monitor to quantify exposure to pollutants in residential environments," *Journal of Sensors and Sensor Systems*, vol. 7, no. 1, pp. 373–388, 2018.

[3] C. Liñán, Y. del Rosal, F. Carrasco, I. Vadillo, J. Benavente, and L. Ojeda, "Highlighting the importance of transitional ventilation regimes in the management of Mediterranean show caves (Nerja-Pintada system, southern Spain)," *Science of the Total Environment*, vol. 631-632, pp. 1268–1278, 2018.

[4] M. D. Rowberry, X. Martí, C. Frontera, M. J. Van De Wiel, and M. Briestenský, "Calculating flux to predict future cave radon concentrations," *Journal of Environmental Radioactivity*, vol. 157, pp. 16–26, 2016.

[5] M. Alvarez-Gallego, E. Garcia-Anton, A. Fernandez-Cortes, S. Cuezva, and S. Sanchez-Moral, "High radon levels in

subterranean environments: monitoring and technical criteria to ensure human safety (case of Castañar cave, Spain)," *Journal of Environmental Radioactivity*, vol. 145, pp. 19–29, 2015.

[6] A. Gregorič, J. Vaupotič, and F. Gabrovšek, "Reasons for large fluctuation of radon and CO₂ levels in a dead-end passage of a karst cave (Postojna Cave, Slovenia)," *Natural Hazards and Earth System Sciences*, vol. 13, no. 2, pp. 287–297, 2013.

[7] A. Fernandez-Cortes, S. Cuezva, E. Garcia-Anton et al., "Changes in the storage and sink of carbon dioxide in subsurface atmospheres controlled by climate-driven processes: the case of the Ojo Guareña karst system," *Environmental Earth Sciences*, vol. 74, no. 12, pp. 7715–7730, 2015.

[8] J. Somlai, J. Hakl, N. Kávási, G. Szeiler, P. Szabó, and T. Kovács, "Annual average radon concentration in the show caves of Hungary," *Journal of Radioanalytical and Nuclear Chemistry*, vol. 287, no. 2, pp. 427–433, 2011.

[9] European Council Directive, "2013/59/Euratom on basic safety standards for protection against the dangers arising from exposure to ionising radiation and repealing Directives 89/618/Euratom, 90/641/Euratom, 96/29/Euratom, 97/43/Euratom and 2003/122/Euratom," *Official Journal of the European Journal*, vol. L13, no. 57, pp. 1–73, 2014.

[10] EH40/2005, "Workplace exposure limits," *HSE Books*, 2018, October 2019, http://www.hse.gov.uk/pUbns/priced/eh40.pdf.

[11] D. T. Mihailović, M. Krmar, G. Mimić et al., "A complexity analysis of ^{222}Rn concentration variation: a case study for Domica cave, Slovakia for the period June 2010-June 2011," *Radiation Physics and Chemistry*, vol. 106, pp. 88–94, 2015.

[12] J. L. U. Baldini, L. M. Baldini, F. McDermott, and N. Clipson, "Carbon dioxide sources, sinks, and spatial variability in shallow temperate zone caves: evidence from Ballynamintra cave, Ireland," *Journal of Cave and Karst Studies*, vol. 68, no. 1, pp. 4–11, 2006.

[13] Y. Kuzyakov, "Sources of CO_2 efflux from soil and review of partitioning methods," *Soil Biology and Biochemistry*, vol. 38, no. 3, pp. 425–448, 2006.

[14] N. Nickerson and D. Risk, "Physical controls on the isotopic composition of soil-respired CO_2," *Journal of Geophysical Research*, vol. 114, no. G1, 2009.

[15] A. Fernandez-Cortes, J. M. Calaforra, and F. Sánchez-Martos, "Hydrogeochemical processes as environmental indicators in drip water: study of the Cueva del Agua (Southern Spain)," *International Journal of Speleology*, vol. 37, no. 1, pp. 41–52, 2008.

[16] S. Milanolo and F. Gabrovšek, "Estimation of carbon dioxide flux degassing from percolating waters in a karst cave: case study from Bijambare cave, Bosnia and Herzegovina," *Chemie der Erde - Geochemistry*, vol. 75, no. 4, pp. 465–474, 2015.

[17] N. Peyraube, R. Lastennet, A. Denis, P. Malaurent, N. Houillon, and J. D. Villanueva, "Determination and quantification of major climatic parameters influencing the CO_2 of Lascaux Cave," *Theoretical and Applied Climatology*, vol. 133, no. 3-4, pp. 1291–1301, 2018.

[18] A. Fernandez-Cortes, S. Sanchez-Moral, S. Cuezva, J. Cañaveras, and R. Abella, "Annual and transient signatures of gas exchange and transport in the Castañar de Ibor cave (Spain)," *International Journal of Speleology*, vol. 38, no. 2, pp. 153–162, 2009.

[19] J. Benavente, I. Vadillo, C. Liñán, Y. del Rosal, and F. Carrasco, "Influence of the ventilation of a karst show cave on the surrounding vadose CO_2 reservoir (Nerja, South Spain)," *Environmental Earth Sciences*, vol. 74, no. 12, pp. 7731–7740, 2015.

[20] C. Pla, J. J. Galiana-Merino, S. Cuezva, A. Fernandez-Cortes, J. C. Cañaveras, and D. Benavente, "Assessment of CO_2 dynamics in subsurface atmospheres using the wavelet approach: from cavity–atmosphere exchange to anthropogenic impacts in Rull cave (Vall d'Ebo, Spain)," *Environmental Earth Sciences*, vol. 75, no. 5, p. 446, 2016.

[21] M. Lang, J. Faimon, P. Pracný, and S. Kejíková, "A show cave management: anthropogenic CO_2 in atmosphere of Výpustek Cave (Moravian Karst, Czech Republic)," *Journal for Nature Conservation*, vol. 35, pp. 40–52, 2017.

[22] S. Cuezva, A. Fernandez-Cortes, D. Benavente, P. Serrano-Ortiz, A. S. Kowalski, and S. Sanchez-Moral, "Short-term CO_2(g) exchange between a shallow karstic cavity and the external atmosphere during summer: role of the surface soil layer," *Atmospheric Environment*, vol. 45, no. 7, pp. 1418–1427, 2011.

[23] S. Peng, Q. Hu, and S. Hamamoto, "Diffusivity of rocks: gas diffusion measurements and correlation to porosity and pore size distribution," *Water Resources Research*, vol. 48, no. 2, article W02507, 2012.

[24] K. E. O'Brien, D. Risk, D. Rainham, and A. M. O'Beirne-Ryan, "Using field analogue soil column experiments to quantify radon-222 gas migration and transport through soils and bedrock of Halifax, Nova Scotia, Canada," *Environmental Earth Sciences*, vol. 72, no. 7, pp. 2607–2620, 2014.

[25] C. Pla, S. Cuezva, J. Martinez-Martinez et al., "Role of soil pore structure in water infiltration and CO_2 exchange between the atmosphere and underground air in the vadose zone: a combined laboratory and field approach," *Catena*, vol. 149, Part 1, pp. 402–416, 2017.

[26] J. D. Jabro, "Water vapor diffusion through soil as affected by temperature and aggregate size," *Transport in Porous Media*, vol. 77, no. 3, pp. 417–428, 2009.

[27] T. K. K. C. Deepagoda, P. Moldrup, P. Schjønning, L. W. de Jonge, K. Kawamoto, and T. Komatsu, "Density-corrected models for gas diffusivity and air permeability in unsaturated soil," *Vadose Zone Journal*, vol. 10, no. 1, pp. 226–238, 2011.

[28] H. Ranaivomanana, J. Verdier, A. Sellier, and X. Bourbon, "Prediction of relative permeabilities and water vapor diffusion reduction factor for cement-based materials," *Cement and Concrete Research*, vol. 48, pp. 53–63, 2013.

[29] A. J. Kowalczk and P. N. Froelich, "Cave air ventilation and CO_2 outgassing by radon-222 modeling: how fast do caves breathe?," *Earth and Planetary Science Letters*, vol. 289, no. 1-2, pp. 209–219, 2010.

[30] E. Garcia-Anton, S. Cuezva, A. Fernandez-Cortes, D. Benavente, and S. Sanchez-Moral, "Main drivers of diffusive and advective processes of CO_2-gas exchange between a shallow vadose zone and the atmosphere," *International Journal of Greenhouse Gas Control*, vol. 21, pp. 113–129, 2014.

[31] C. Sainz, D. Rábago, S. Celaya et al., "Continuous monitoring of radon gas as a tool to understand air dynamics in the cave of Altamira (Cantabria, Spain)," *Science of the Total Environment*, vol. 624, pp. 416–423, 2018.

[32] F. Perrier, P. Richon, U. Gautam, D. R. Tiwari, P. Shrestha, and S. N. Sapkota, "Seasonal variations of natural ventilation and radon-222 exhalation in a slightly rising dead-end tunnel," *Journal of Environmental Radioactivity*, vol. 97, no. 2-3, pp. 220–235, 2007.

[33] S. F. M. Breitenbach, F. A. Lechleitner, H. Meyer, G. Diengdoh, D. Mattey, and N. Marwan, "Cave ventilation and rainfall signals in dripwater in a monsoonal setting - a monitoring study from NE India," *Chemical Geology*, vol. 402, pp. 111–124, 2015.

[34] M. Ota and H. Yamazawa, "Forest floor CO_2 flux estimated from soil CO_2 and radon concentrations," *Atmospheric Environment*, vol. 44, no. 36, pp. 4529–4535, 2010.

[35] L. K. McDonough, C. P. Iverach, S. Beckmann et al., "Spatial variability of cave-air carbon dioxide and methane concentrations and isotopic compositions in a semi-arid karst environment," *Environmental Earth Sciences*, vol. 75, no. 8, p. 700, 2016.

[36] J. Lario, S. Sánchez-Moral, J. C. Cañaveras, S. Cuezva, and V. Soler, "Radon continuous monitoring in Altamira Cave (northern Spain) to assess user's annual effective dose," *Journal of Environmental Radioactivity*, vol. 80, no. 2, pp. 161–174, 2005.

[37] A. Denis and F. Cremoux, "Using the entropy of curves to segment a time or spatial series," *Mathematical Geology*, vol. 34, no. 8, pp. 899–914, 2002.

[38] F. Perrier and P. Richon, "Spatiotemporal variation of radon and carbon dioxide concentrations in an underground quarry: coupled processes of natural ventilation, barometric pumping and internal mixing," *Journal of Environmental Radioactivity*, vol. 101, no. 4, pp. 279–296, 2010.

[39] A. Fernandez-Cortes, S. Sanchez-Moral, S. Cuezva, D. Benavente, and R. Abella, "Characterization of trace gases' fluctuations on a 'low energy' cave (Castañar de Íbor, Spain) using techniques of entropy of curves," *International Journal of Climatology*, vol. 31, no. 1, pp. 127–143, 2011.

[40] I. Daubechies, *Ten Lectures on Wavelets*, Society for Industrial and Applied Mathematics, Philadelphia, PA, USA, 1992.

[41] G. A. Kaiser, *A Friendly Guide to Wavelets*, Birkhäuser Basel, 2011.

[42] M. V. Wickerhauser, *Adapted Wavelet Analysis from Theory to Software*, A K Peters/CRC Press, 1996.

[43] G. Strang and T. Nguyen, *Wavelets and Filter Banks*, Wellesley-Cambridge Press, 1997.

[44] J. J. Galiana-Merino, C. Pla, A. Fernandez-Cortes, S. Cuezva, J. Ortiz, and D. Benavente, "EnvironmentalWaveletTool: continuous and discrete wavelet analysis and filtering for environmental time series," *Computer Physics Communications*, vol. 185, no. 10, pp. 2758–2770, 2014.

[45] H. Ghahremanzadeh, R. Noori, A. Baghvand, and T. Nasrabadi, "Evaluating the main sources of groundwater pollution in the southern Tehran aquifer using principal component factor analysis," *Environmental Geochemistry and Health*, vol. 40, no. 4, pp. 1317–1328, 2018.

[46] M. Azam, S. Maeng, H. Kim, S. Lee, and J. Lee, "Spatial and temporal trend analysis of precipitation and drought in South Korea," *Water*, vol. 10, no. 6, p. 765, 2018.

[47] D. Benavente, C. Pla, N. Cueto et al., "Predicting water permeability in sedimentary rocks from capillary imbibition and pore structure," *Engineering Geology*, vol. 195, pp. 301–311, 2015.

[48] I. T. Jolliffe, *Pincipal Component Analysis*, Springer-Verlag, New York, NY, USA, 2002.

[49] C. Pla, S. Cuezva, E. Garcia-Anton et al., "Changes in the CO_2 dynamics in near-surface cavities under a future warming scenario: factors and evidence from the field and experimental findings," *Science of the Total Environment*, vol. 565, pp. 1151–1164, 2016.

[50] AEMET-IM, *Iberian Climate Atlas. Air Temperature and Precipitation (1971-2000) in Agencia Estatal de Metereologia (España)*, Instituto de Metereologia, Portugal, 2011, http://www.aemet.es/es/conocermas/publicaciones/detalles/Atlas-climatologico.

[51] E. Garcia-Anton, S. Cuezva, A. Fernandez-Cortes et al., "Abiotic and seasonal control of soil-produced CO_2 efflux in karstic ecosystems located in oceanic and Mediterranean climates," *Atmospheric Environment*, vol. 164, pp. 31–49, 2017.

[52] A. Grinsted, J. C. Moore, and S. Jevrejeva, "Application of the cross wavelet transform and wavelet coherence to geophysical time series," *Nonlinear Processes in Geophysics*, vol. 11, no. 5/6, pp. 561–566, 2004.

[53] J. Valdes-Abellan, C. Pla, M. Fernandez-Mejuto, and J. M. Andreu, "Validating the KAGIS black-box GIS-based model in a Mediterranean karst aquifer: case of study of Mela aquifer (SE Spain)," *Hydrological Processes*, vol. 32, no. 16, pp. 2584–2596, 2018.

[54] J. G. Proakis and D. G. Manolakis, *Digital Signal Processing: Principles, Algorithms and Applications*, Prentice-Hall/Pearson Education, Englewood Cliffs, NJ, USA, 2007.

[55] D. Labat, R. Ababou, and A. Mangin, "Multiresolution cross-analysis of rainfall rates and karstic spring runoffs," *Comptes Rendus Geoscience*, vol. 334, no. 8, pp. 551–556, 2002.

[56] J.-B. Charlier, B. Ladouche, and J.-C. Maréchal, "Identifying the impact of climate and anthropic pressures on karst aquifers using wavelet analysis," *Journal of Hydrology*, vol. 523, pp. 610–623, 2015.

[57] M. Prelovšek, S. Šebela, and J. Turk, "Carbon dioxide in Postojna Cave (Slovenia): spatial distribution, seasonal dynamics and evaluation of plausible sources and sinks," *Environmental Earth Sciences*, vol. 77, no. 7, p. 289, 2018.

[58] S. Šebela and J. Turk, "Črna Jama as a cold air trap cave within Postojna Cave, Slovenia," *Theoretical and Applied Climatology*, vol. 134, no. 3-4, pp. 741–751, 2018.

[59] F. Bourges, P. Genthon, A. Mangin, and D. D'Hulst, "Microclimates of l'Aven d'Orgnac and other French limestone caves (Chauvet, Esparros, Marsoulas)," *International Journal of Climatology*, vol. 26, no. 12, pp. 1651–1670, 2006.

[60] S. Frisia, I. J. Fairchild, J. Fohlmeister, R. Miorandi, C. Spötl, and A. Borsato, "Carbon mass-balance modelling and carbon isotope exchange processes in dynamic caves," *Geochimica et Cosmochimica Acta*, vol. 75, no. 2, pp. 380–400, 2011.

[61] D. O. Breecker, A. E. Payne, J. Quade et al., "The sources and sinks of CO_2 in caves under mixed woodland and grassland vegetation," *Geochimica et Cosmochimica Acta*, vol. 96, pp. 230–246, 2012.

[62] J. Pu, D. Yuan, H. Zhao, and L. Shen, "Hydrochemical and PCO2 variations of a cave stream in a subtropical karst area, Chongqing, SW China: piston effects, dilution effects, soil CO_2 and buffer effects," *Environmental Earth Sciences*, vol. 71, no. 9, pp. 4039–4049, 2014.